Three-Dimensional Digital Subtraction Angiography

(디지탈 血管 造影術 映像의 3次元的 解析)

李承智*, 金喜贊*, 閔丙九*, 李泰洙*,

李忠雄**, 朴在亨***, 韓萬靑***

(Seung-Ji Lee, Hee-Chan Kim, Byoung-Goo Min, Tae-Soo Lee,

Choong-Woong Lee, Jae-Hyung Park and Man-Chung Han)

要　約

본 논문에서는 디지탈 감산 기법을 이용한 양면 혈관 조영술 영상에서의 대응점 결정을 위하여 조영제 말단 추적 알고리즘을 사용하였고, 이 대응점 정보로부터 혈관의 3차원 영상을 재구성하는 과정을 확립하였으며, 개를 이용한 실험 결과도 포함되어 있다. 저자들에 의해 개발된 본 방법의 정확성을 입증하기 위해 사각에서 잡은 혈관 조영상과 계산을 통해 재구성된 영상을 비교하여 좋은 결과를 얻었다. 본 논문에서는 3가지의 새로운 알고리즘을 개발, 또는 응용하였는바, 첫째는, 순차적인 영상에서 조영제의 말단은 어느 투영면에서도 동일한 형태를 갖게 되므로, 상호 상관 계수의 접합법을 이용하여 조영제 말단을 추적해 가는 알고리즘이고, 둘째는, 기준좌표계에서 시선 좌표계로의 전환을 4×4행렬 하나로 표시한 단순화 투시 변환 행렬의 구성이며, 셋째는, 조영제 말단 추적법이 적용될 수 없는 작은 혈관 영상에서의 대응점 확립을 위한 보조알고리즘의 적용이 그것이다. 또한 본 방법은 3차원 공간상에서의 조영제 말단 이동거리에 대한 정보로부터 혈류 속도의 측정에도 이용될 수 있다.

Abstract

A dye-edge tracking algorithm was used to determine the corresponding points in the two images (anterior-posterior and lateral) of the digital subtraction biplane angiography. This correspondence was used to reconstruct three dimensional images of cerebral artery in a dog experiment. The method was tested by comparing the measured image of oblique view with the computed reconstructed image. For the present study, we have developed three new algorithms. The first algorithm is to determine the corresponding dye-edge points using the fact the dye density at the moving edge shows the same changing pattern in the two projection views. This moving pattern of dye-edge density is computed using a matching method of cross-correlation for the two sequential frames' dye density. The second algorithm is for simplified perspective transformation, and the third one is to identify the specific corresponding points on the small vessels. The present method can be applied to compute the blood velocity using the dye-edge displacement and the three-dimensional distance data.

*正会員, 서울대학교 医科大学 医工学科
　(Dept. of Biomedical Eng., Seoul National Univ.)
***正会員, 서울大学校 医科大学 放射線科
　(Dept. of Diagnostic Radiology, Seoul National Univ.)
**正会員, 서울大学校 工科大学 電子工学科
　(Dept. of Electronics Eng., Seoul National Univ.)
接受日字: 1982年 9月 24日

I. Introduction

Digital subtraction angiography(DSA)[1],[2] is a relatively new diagnostic tool for early detection of vascular diseases. By displaying the blood vessel image without background interference, DSA can provide an improved blood vessel image with reduced amount of dye

injection in arterial angiography. Also, this method can be used as a noninvasive technique with intravenous injection of radiopaque dye. Another promising area of DSA application is a quantitative functional study of physiological state, using the changes of dye density in sequential frames[3].

As a preliminary study for application of DSA on the blood flow dynamics, we present a new method of reconstructing three-dimensional (3-D) angiographic images from the biplane two-dimensional (2-D) angiographic data. Especially we have developed a method of utilizing the changes of dye density at its moving edge in sequential image frames to find the corresponding vessel points between two images.

In previous methods of conventional angiographic system, the corresponding points were determined manually for each point, or a priori information of the feature points was used to estimate the correspondence[4].

In addition to the above improvement, we also applied a new simplified perspective transformation method for displaying 3-D data in 2-D plane, and evaluated an algorithm of finding a corresponding point in small size vessels.

II. Computer Algorithms

1. Three-Dimensional Coordinate Reconstruction

The projection of a point in 3-Dimensional space to a 2-Dimensional image plane can be represented by a transformation matrix, T, in the homogeneous coordinate system[5] as follows;

$$[X,Y,Z,1] \times \underbrace{\begin{pmatrix} T_{11} & T_{12} & T_{13} \\ T_{21} & T_{22} & T_{23} \\ T_{31} & T_{32} & T_{33} \\ T_{41} & T_{42} & T_{43} \end{pmatrix}}_{T} = [x',y',w'] = w'[U,V,1] \quad (1)$$

where (X,Y,Z) is the position in a 3-D space,
(x',y') is the 2-D position,

w' is an arbitrary scale factor,
(U,V) is the normalized 2-D position.

In Eq. (1), the twelve elements of T matrix, Tij, are the characteristic parameters determining the projection of any points in 3-D space to 2-D plane. Thus, any 3D-to2-D projection and its inverse can be obtained using Tij parameters, where Tij can be computed from 3D-to2D projection data for at least 5½ points.[6] In the present study, the three dimensional position and its projection data of twelve reference points of lead pellets inside a plastic phantom were used to compute Tij. Using the computed Tij and two 2-D projection position data of a point, one can estimate the position in 3-D space by the least square error method.[7]

2. Algorithms for Detecting Dye-edge Points

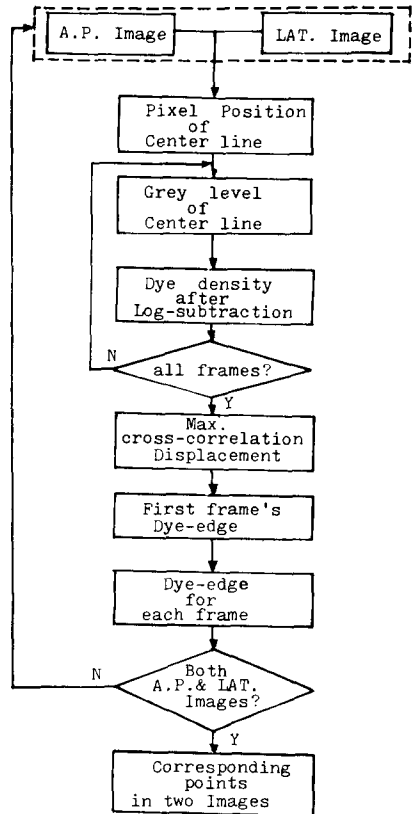The correspondence of a point in the an-

Fig. 1. A flow-chart of edge-tracking algorithm.

terior-posterior (AP) and lateral (LAT) images of the biplane angiography is obtained using the fact that the dye density at the moving edge shows the same changing pattern in the two projection views. This moving pattern of dye-edge density is evaluated using a matching method of cross-correlation for the two sequential frames' dye density.

Detailed algorithm is shown in Fig. 1. First, the region of interest (ROI) of the vessel is determined after logarithmic processing and subtraction procedure between the completely dye-filled frame's image (the last frame) and the mask image of pre-injection. Then, the center line is traced along the vessel to provide the pixel position data. The varying dye density data for sequential frames along this center line are used for computation of the cross-correlation coefficient. The dye displacement between the two frame sequences is determined by the pixel difference having the maximal cross-correlation coefficient, as given in the following equation[10], and Fig. 2.

$$\rho_i(k) = \frac{\sum\limits_{n=1}^{N-k}\left\{ D_{i-1}^k(n) - \bar{D}_{i-1}\right\}\left\{ D_i(n) - \bar{D}_i\right\}}{\sqrt{\sum\limits_{n=1}^{N-k}\left\{ D_{i-1}(n) - \bar{D}_{i-1}\right\}^2 \sum\limits_{n=1}^{N-k}\left\{ D_i(n) - \bar{D}_i\right\}^2}}$$

(2)

$$\text{and} \quad \bar{D}_i = \frac{1}{N-k}\sum\limits_{n=1}^{N-k} D_i(n)$$

where i; the frame sequence number of the present image frame,

n; the pixel position number of the center line in a given frame,

N; the total pixel numbers of the center line in one frame,

$D_i(n)$; the relative dye density at the n-th pixel position in the i-th frame

k; the pixel shift variable in computing cross-correlation.

For the relative dye density profiles of two sequential image frames, $D_i(n)$ and $D_{i-1}(n)$ in Fig. 2, the cross-correlation coefficients, $\rho_i(k)$, are computed in Eq. (1) for each k. Then, as shown in Fig. 2, the $\rho_i(k)$ has the max. value when the pixel shift variable of cross-correlation, k, equals the dye-edge displacement between the two sequential frames. Thus, by selecting k_m which provides the maximum value of $\rho_i(k)$, we can estimate the dye-edge displacement.

Then, the dye-edge position of the current frame is computed by adding this pixel number of dye displacement to the prior frame's dye edge position.

The above procedures are repeated for both lateral and anterior images, and the dye-edge points of two images are considered as the corresponding points at each frame.
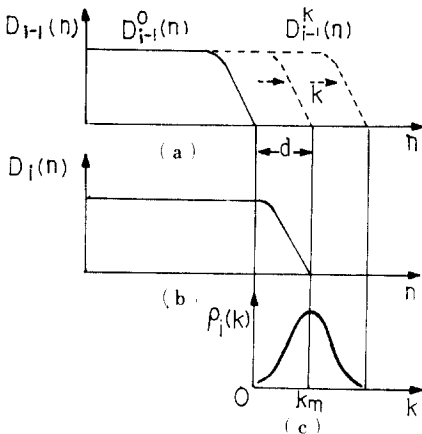

Fig. 2. Computation of the dye-edge displacement using the cross-correlation method.
In (a), $D_{i-1}^0(n)$ shows the relative dye density profile against the pixel position in the previous frame and $D_{i-1}^k(n)$ is the same profile shifted by k pixels. Fig. 2. (b) shows the present frame's dye density profile against the pixel position, (c) shows the computed cross-correlation between the above two profiles as a function of shift variable, k. The maximal cross-correlation point of k_m provides the estimated value of the dyedge displacement of "d".

3. Complementary methods for determination of corresponding points on the vessel

When the accuracy of the above cross-correlation method is low due to scattering noise in small size vessels, the projection matrix (T) and the projection data in one image are used to identify the corresponding vessel points of the other image, using the following complementary method[6]. Also this method can be used to determine any corresponding points located between two neighboring dye-edge points.

When Tij and T'ij are the projection trans-from matrices for two 2-D biplane images, and (U,V) and (U',V') are their projected position data for a given point, U' and V' must satisfy the following line equation:

$$U' = MV' + N \tag{3}$$

where

$$M = \frac{AD - BC}{AD' - BC'} \qquad N = \frac{C}{A} + M \cdot \frac{C'}{A}$$

$A = T'_{13} + T'_{23}s_1 + T'_{33}s_2 \qquad B = T'_{23}t_1 + T'_{33}t_2 + T'_{43}$

$C = T'_{11} + T'_{21}s_1 + T'_{31}s_2 \qquad D = T'_{21}t_1 + T'_{31}t_2 + T'_{41}$

$C' = T'_{12} + T'_{22}s_1 + T'_{32}s_2 \qquad D' = T'_{22}t_1 + T'_{32}t_2 + T'_{42}$

$$s_1 = \frac{a_2c_1 - a_1c_2}{b_1c_2 - b_2c_1} \qquad s_2 = \frac{a_1b_2 - a_2b_1}{b_1c_2 - b_2c_1}$$

$$t_1 = \frac{c_1d_2 - c_2d_1}{b_1c_2 - b_2c_1} \qquad t_2 = \frac{b_2c_1 - b_1c_2}{b_1c_2 - b_2c_1}$$

$a_1 = T_{11} - T_{13}U \qquad a_2 = T_{12} - T_{13}V$

$b_1 = T_{21} - T_{23}U \qquad b_2 = T_{22} - T_{23}V$

$c_1 = T_{31} - T_{33}U \qquad c_2 = T_{32} - T_{33}V$

$d_1 = T_{41} - T_{43}U \qquad d_2 = T_{42} - T_{43}V$

When the corresponding vessels in the two images are known, this line equation can be used to identify a specific corresponding vessel point on the second image for any given points in the first image as shown in Fig. 3.

4. Perspective View

We also developed a new simplified perspective transformation method in presenting a perspective view from the reconstructed 3-D
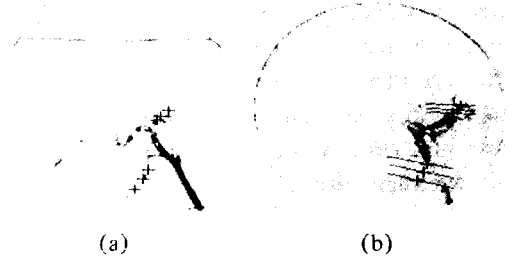

(a)   (b)

Fig. 3. A complementary method was used to determine the corresponding points in small size vessels. Six points in A.P. image (b) corresponding to the points in LAT. image (a) were determined by the crossing points of the vessels and the lines.

image data for any observer locations and viewing angles.

Using a geometrical manipulation, the relation between the eye coordinate (X_e, Y_e, Z_e) and the world coordinate (X_w, Y_w, Z_w) is given as follows;

$$[X_e, Y_e, Z_e, 1] = [X_w, Y_w, Z_w, 1] \cdot$$

$$\begin{pmatrix} -\dfrac{b}{R^2} & -\dfrac{ac}{R_1 R_2} & -\dfrac{a}{R_1} & 0 \\[2mm] \dfrac{a}{R_2} & -\dfrac{bc}{R_1 R_2} & -\dfrac{b}{R_1} & 0 \\[2mm] 0 & \dfrac{R_2}{R_1} & -\dfrac{c}{R_1} & 0 \\[2mm] 0 & 0 & R_1 & 1 \end{pmatrix} \tag{4}$$

where (a,b,c) is the observer's position in world coordinate,

$$R_1 = (a^2 + b^2 + c^2)^{1/2}$$
$$R_2 = (a^2 + b^2)^{1/2}$$

Then, the eye coordinate data can be used to compute the screen coordinates (X_s, Y_s) using a simple triangular relation.[5] Also, assuming a cylindrically symmetric vessel structure, the vessel can be displayed in its real size using the vessel diameter of the projection image.

The algorithms for 3-D reconstruction, dye-edge detection, and perspective display are summarized in the flow-chart of Fig. 4.
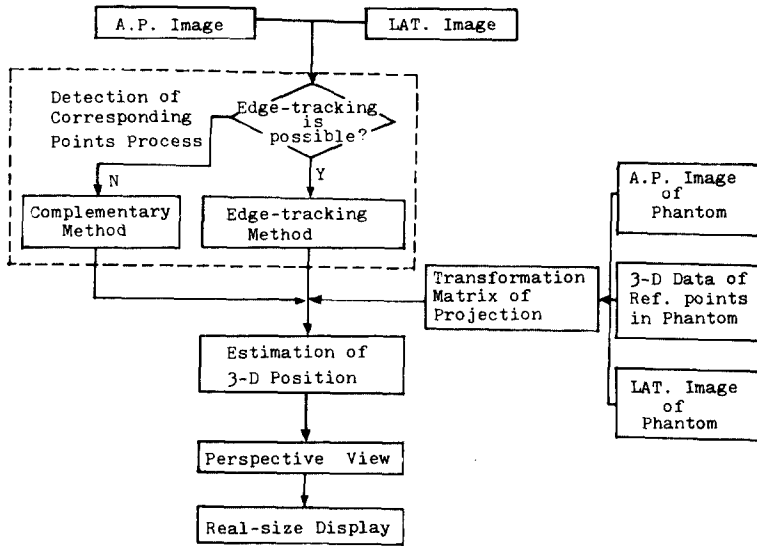
Fig. 4. A flow-chart of the 3-dimensional reconstruction algorithm with dye-edge tracking method.

III. Experiment and Methodology

1. Cerebral Biplane Angiography

The present algorithms were tested in cerebral artery biplane angiography of a dog weighing 19-Kg. A catheter was located in ascending aorta after insertion through the femoral artery. A bolus of radiopaque dye was injected using a power injector (Medrad, Mark IV) at an injection rate of 5ml/sec for total amount of 7 ml.

2. Measurement Technique

Our own DSA system is shown in the system block diagram of Fig. 5 which consists of a X-ray generator (G.E., MSI-1250/V, 1000 MA), image intensifier (6″-9″ Circular, Cesium Iodide), plumbicon camera and two VTRs (3/4″, Victor, Umatic). The recorded video data at the frame rate of 30 frames/sec was digitally processed using a Image Frame store (Colorado Video Inc. with 256x256 6bits), and analyzed using a MINC-11 computer.
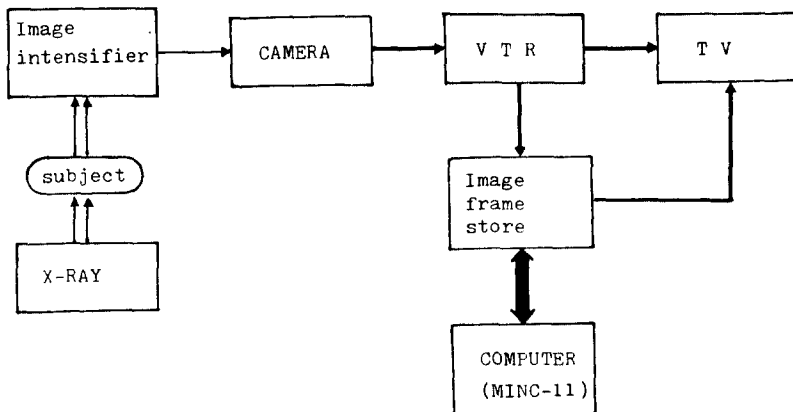

Fig. 5. A block diagram of DSA system, developed previously by our group and used for the present study.

Dye-edge tracking for twenty frame's data was accomplished using the method described above. The first dye-edge point was determined by comparing the decreasing dye density pattern in A.P. and LAT. images.

The 3-D reconstruction and its perspective display were obtained using the previously described method.

The overall procedure is illustrated in Fig. 13.

IV. Results

Fig. 6 shows the dye-filled image for A.P., and LAT. views, and Fig. 7 shows the cerebral artery image after digital logarithmic substraction process between the mask images and the dye-filled images.

(a) AP image   (b) LAT image

Fig. 6. Dye-filled images of canine cerebral artery.

(a) AP image   (b) LAT image

Fig. 7. The blood vessel images after logarithmic and subtraction process.

Changes of the grey-level data for 200 pixels along the vessel's center line are shown in Fig. 8 for twenty LAT. image frame sequences. After performing log-subtraction between the mask image and each frame image, the center line's dye density data are shown in Fig. 9. These data were used for
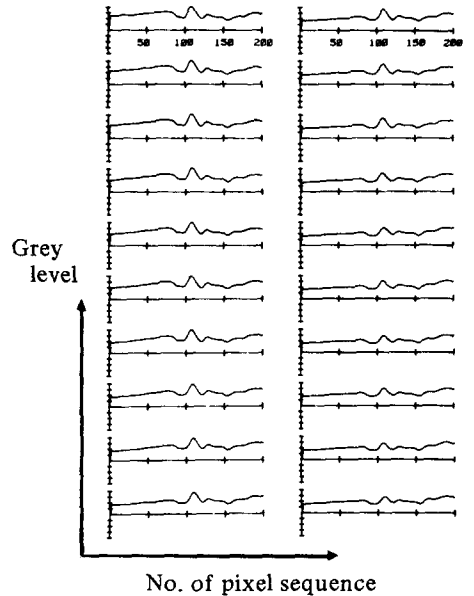

Fig. 8. Grey level for the center line of Fig. (6) in 20 frame sequences.
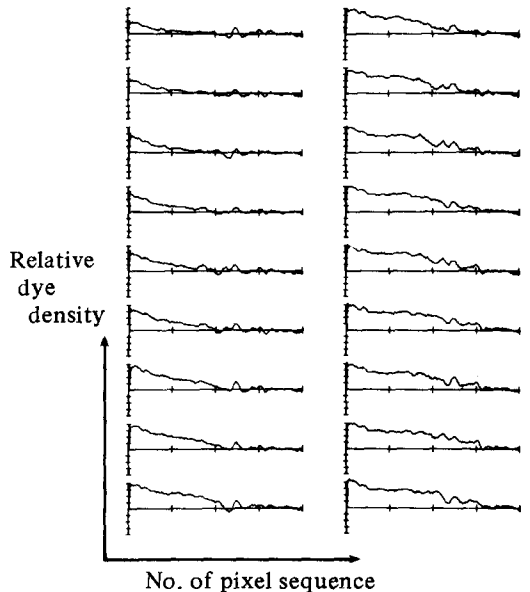

Fig. 9. Changes of dye density, as computed after log-subtraction of the grey level data of Fig. (7).

computation of cross-correlation coefficients.

The fluctuation of grey-level data in Fig. 8 might be caused by the X-ray scattering. This fluctuation decreased significantly in the dye density data of Fig. 9 after log-subtraction
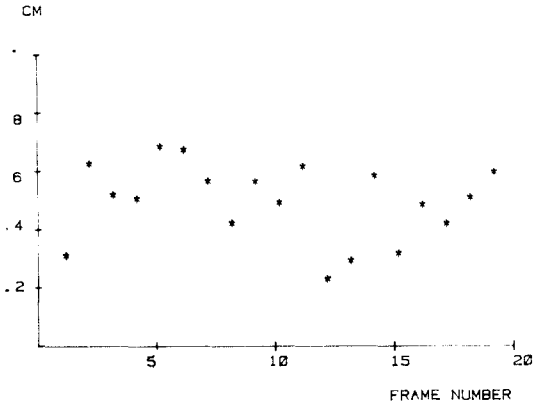
Fig. 10. Dye-edge displacement between the sequential frames, as measured in actual traveling distance for each frame.
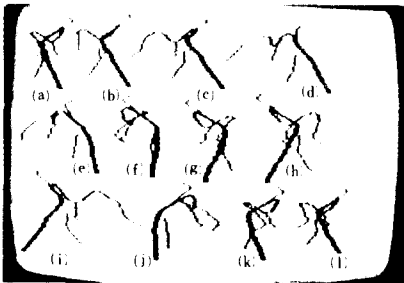

Fig. 11. Twelve perspective views of the reconstructed 3-D images for different observing angles, as viewed in 30° interval.
(a) and (b) are A.P. and LAT. images respectively. Approximate mirror images are obtained in (c) and (i), (f) and (j), and (g) and (k).

Fig. 12. Comparison of the measured and the computed images;
(a), (b) are original oblique views in biplane angiography.
(c), (d) are the computed oblique views corresponding to (a) and (b), respectively,
(e) is the computed axial view,
(f) is the computed image for the same angle as the measured A.P. image,
(g) is the computed image for the same angle as the measured LAT. image.

V. Discussion

In this paper, the dye-edge tracking algorithm was used to determine the corresponding points in two images (A.P. & LAT.) of the digital biplane angiography. This correspondence was used for three-dimensional reconstruction of carotid arteriography. The method was tested by comparing the measured image of oblique view and the computed image for the same viewing location and angle.

The present method has the following characteristics for its future clinical applications; First, using the computed perspective views, the clinicians can determine the optimal angle difference for biplane angiography to locate the specific lesions, such as the occlusion

process.

The displacement distance of the moving dye-edge at each pixel is shown in Fig. 10. Due to the pulsatile characteristics of the cerebral blood flow, it is shown that the displacement distance is different for each frame.

Fig. 11 shows the perspective views for different observer's viewing angles. The validity of the present study can be shown in Fig. 12 where the computed oblique view is compared to the measured oblique image.
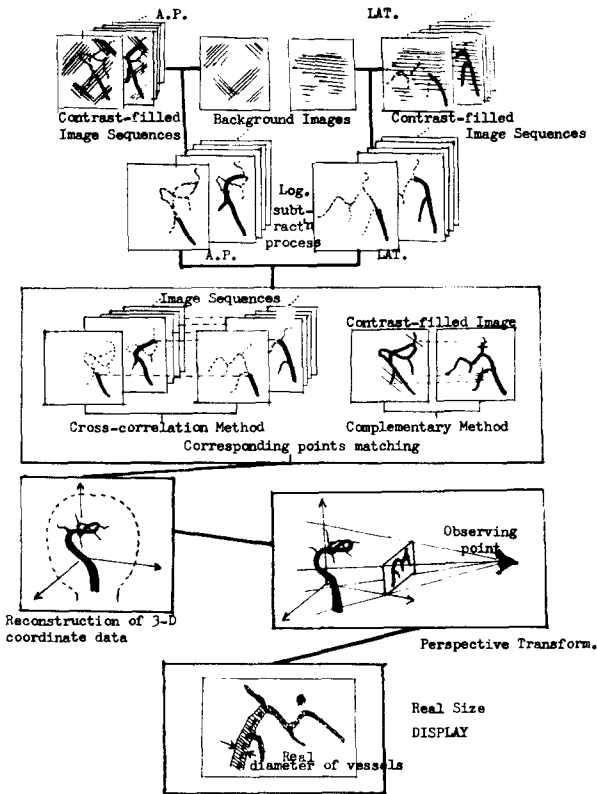
Fig. 13. Illustration of the overall procedure.

points. Second, the neighboring or the overlaying vessels can be separated for selective angiography using the present method when the arrival times of the contrast media are different for these vessels. Also, any vessels parallel to the line of the X-ray source to the image intensifier can be easily located by the stationary dye-edge points. Third, the pulsatile blood flow velocity and its distribution may be measured by using the dye-edge displacement in the peripheral arteries with slow flow velocity[9]. Since the digital subtraction angiography can be used noninvasively, the blood flow velocity measured from the dye-edge tracking system may be used as important clinical data in diagnosis of the vascular diseases.

The estimation error for 3-D reconstruction could be caused by the noise effects existing in the digital subtraction angiographic system.

The noise sources include the scatter in the patient, the veiling glare in the image intensifier, the beam hardening effects, and the patient's motion artifacts. In addition to these noise sources problems, the present cross-correlation method requires the same dye-edge profiles in the sequential frames. In the present study of cerebral artery, it is shown that these conditions are satisfied to provide the dye-edge displacement.

We also plan to convert our present 256x256 pixel size to 512x512 pixels to improve the original image resolution, and we are evaluating various noise reduction techniques[8] to improve our DSA image quality.

Reference

[1] P.C. Christenson, T.W. Ovitt, et al., "Intravenous angiography using digital video subtraction: intravenous cervico-cerebrovascular angiography," AJR, vol. 135, no. 12, pp. 1145-1152, 1980.

[2] T.W. Ovitt, P.C. Christenson, H.D. Fisher, et al., "Intravenous angiography using digital video subtraction: X-ray imaging system," *AJR*, vol. 135, no. 12, pp. 1141-1144, 1980.

[3] H.C. Smith, R.A. Robb, E.H. Wood, *Myocardial Blood Flow: Roentgen Video-densitometry Techniques*. Conf. on Cardiovascular Imaging & Image Processing: Theory & Practice-1975, pp. 225-232, 1975.

[4] R.E. Sayer, J.M. Rubin, et al., *Quantitative Three-Dimensional Angiograms: Applications, Including Augmentation of Computed Tomograms*. Proc. 6th Conference on Computer Application in Rad. & Computer/Aided Analysis of Radiological Images, pp. 95-102, 1979.

[5] W.M. Newman & R.F. Sproull, *Principles of Interactive Computer Graphics*. New York: Mcgraw-Hill, 1973.

[6] I.E. Sutherland, "Three-dimensional data input by tablet," *Proc. of the IEEE*, pp. 453-461, Apr. 1974.

[7] L.P. Adams, "X-Ray stereo photogrammetry locating the precise three-dimensional position of image points," *Medical & Biological Engineering & Computing*, vol. 15, no. 5, pp. 569-578, Sep. 1981.

[8] C.G. Show, D.L. Ergun, et al., "A technique of scatter and glare correction for video-densitometric studies in digital subtraction videoangiography," *Radio-* *logy*, vol. 142, no. 1, pp. 209-213, Jan. 1982.

[9] J.H. Bursch, et al., "Assessment of arterial blood flow measurements by digital angiography," *Radiology*, vol. 141, no. 1, pp. 39-47, Oct. 1981.

[10] M.G. Edmund, S.R. Daniel, *Principles of Neurobiological Signal Analysis*. Academic Press, 1976.